CHEMICAL ENGINEERING TRANSACTIONS
VOL. 62, 2017
A publication of AIDIC
The Italian Association of Chemical Engineering
Online at www.aidic.it/cet
Guest Editors: Fei Song, Haibo Wang, Fang He

ISBN 978-88-95608- 60-0; **ISSN** 2283-9216
DOI: 10.3303/CET1762010

Optimization and Microstructure Study of the Reduction of Nickel Smelting Slag Mixed with Calcium Carbide Slag and Coke Dust for Recovering Iron

Shuang Wang[a], Changlong Wang[b,c,d]*, Qunhui Wang[a], Wen Ni[e], Keqing Li[f]

[a]Beijing Key Laboratory on Resource-oriented Treatment of Industrial Pollutant, School of Energy and Environmental Engineering, University of Science and Technology Beijing, Beijing 100083, China
[b]Jiangxi Key Laboratory of Mining Engineering, Jiangxi University of Science and Technology, Ganzhou Jiangxi Province 341000, China
[c]School of Civil Engineering, Hebei University of Engineering, Handan Hebei Province, 056038, China
[d]Tianjin Sunenergy Sega Environmental Science & Technology Co. Ltd, Tianjin 300000, China
[e]Beijing Key Laboratory on Resource-oriented Treatment of Industrial Pollutant, School of Civil and Resource Engineering, University of Science and Technology Beijing, Beijing 100083, China
[f]Key Laboratory of the Ministry of Education of China for High-Efficient Mining and Safety of Metal Mines, School of Civil and Resource Engineering, University of Science and Technology Beijing, Beijing 100083, China
13716996653@139.com

How to treat more industrial solid waste friendly and environmental have become the global issues. In this study, direct reduction-magnetic separation (DRMS) process was employed to recovery iron from the nickel smelting slag (NSS) with calcium carbide slag (CCS) as the additive and coke dust (CD) as the reductant. Response surface methodology (RSM) approach using central composite design (CCD) was adopted for optimizing the effects of reduction temperature, reduction time and CCS dosage on the iron content of iron concentrate powder (ICP) and iron recovery. The results were modeled and the impact factors were evaluated. All the plots show that there were positive correlations between investigated impact factors and responses in a certain range but if exceeded, the positive correlations would be broken down. The overall optimization reaction conditions were converged as around 1287 ºC, 2.8 h and CCS dosage of 57.19 %. Under these proven optimization reaction conditions, the iron content of ICP and iron recovery were reached up to 91.30 % and 95.44 % respectively. The micro phase of reduced samples were investigated by X-ray diffraction analysis (XRD), in reduction process, and the microstructure of reduced samples under the optimal condition were investigated by SEM for further discussion and analyzation. The experimental results and microstructure analysis suggests that utilizing CCS and CD in DRMS process were viable.

1. Introduction

Comprehensive recycling and utilization of industrial solid waste is one of the important measures for industrial sustainable development. One of the known industrial solid wastes from nickel smelters is nickel smelting slag (NSS), which is discharged from smelting furnace and produced about 2 million tons each year in China. The NSS could be utilized as secondary iron-bearing material, because it contains about 30-40 % of iron that can be reduced and recovered by direct reduction-magnetic separation (DRMS) process (Wang et al., 2014). (Mu'azu et al., 2014). It is thought that utilizing of the waste nickel slag may not only reduce iron raw ore material costs and relieve the supply of high quality iron ore for iron-making process, but also eliminated the environmental pollutions and ecological destruction potentially caused by discarding hazardous waste at dump sites in the future. Recovery iron from waste iron-bearing slag or other nonferrous metallurgical slag by DRMS process have been suggested in several research papers (Wang et al., 2015; Wang et al., 2014; Fan et al., 2015; Li et al., 2013). (Jia et al., 2011). The DRMS methods generally include two key processes: pyrometallurgical reduction (PR) and physical separation (PS). In most PR process, the waste slag is mixed with calcium compound such as calcium oxide (CaO) as an additive, binary basicity (mass ratio of CaO and

Please cite this article as: Shuang Wang, Changlong Wang, Qunhui Wang, Wen Ni, Keqing Li, 2017, Optimization and microstructure study of the reduction of nickel smelting slag mixed with calcium carbide slag and coke dust for recovering iron, Chemical Engineering Transactions, 62, 55-60 DOI:10.3303/CET1762010

SiO_2) as a composition regulation index, and coal as a reduction agent. Then, the mixture is roasted at a high temperature of 1373-1673 K (1100-1 400 ºC) for reducing iron-bearing phase to metallic iron.
In this study, the calcium carbide slag (CCS) and coke dust (CD) are investigated as the additive and reductant respectively in DRMS process of NSS for recycling and utilizing the solid waste and lowering economic cost. Furthermore, the previous researches have been conducted the influences of parameters include additive dosage, reduction time and reduction temperature in DRMS process by a sequential series of single factor optimization. However, in consideration of possible interactions of factors and better efficiency, a comprehensive parameters optimization is significantly needed. Thus, based on the response surface method, this study provides new results for evaluating the influence of several parameters, in addition with the verification as well as the analyzation of phase transformations and micro-morphological changes under the optimal condition, which can be used as a reference for the future works in this field.

2. Experimental

2.1 Raw Materials Characteristics

The NSS was obtained from a flash furnace at a nickel smelter in Gansu province, China. And its chemical composition was given in Table 1. The CCS and CD were obtained from Hebei province, which was the largest iron and steel production region in China. The chemical composition of CCS was shown in Table 1 and proximate analysis of CD was presented in Table 2. It can be seen that the main components of NSS are 43.58 % FeO and 39.04 % SiO_2, while the main ingredient contained in CSS was 67.09 % CaO.

Table 1: The chemical compositions of NSS and the CCS (mass fraction, %)

Materials	SiO_2	CaO	MgO	Al_2O_3	Fe_2O_3	FeO	Na_2O	K_2O	P_2O_5	MnO	TiO_2	SO_3	LOI
NNS	39.04	2.36	8.47	2.85	3.77	43.58	0.31	0.23	0.025	0.40	0.15	1.56	1.14
CCS	4.09	67.09	—	2.16	0.04	0.36	0.28	0.13	0.020	0.005	0.076	0.35	25.84

Table 2: Industrial analysis of CD used in the test (mass fraction, %)

Moisture	Ash	Volatile	Fixed carbon	Total sulfur
0.41	12.87	1.30	85.83	0.76

XRD pattern of the NSS was shown in Figure 1(a), which showed the presence of fayalite (Fe_2SiO_4), magnetite (Fe_3O_4)and martensite (Fe-Fe_3C). It indicated that iron mostly occurs in fayalite and magnetite, and some amorphous structures were present because that the nickel slag was cooled and granulated quickly by spraying of water. Figure 1(b) represents XRD patterns of the carbide slag and it clearly had plenty of portlandite ($Ca(OH)_2$), calcite ($CaCO_3$) and calcium aluminum oxide hydrate ($3CaO{\cdot}Al_2O_3{\cdot}6H_2O$), which was consistent with the chemical composition results shown previously in Table 1.

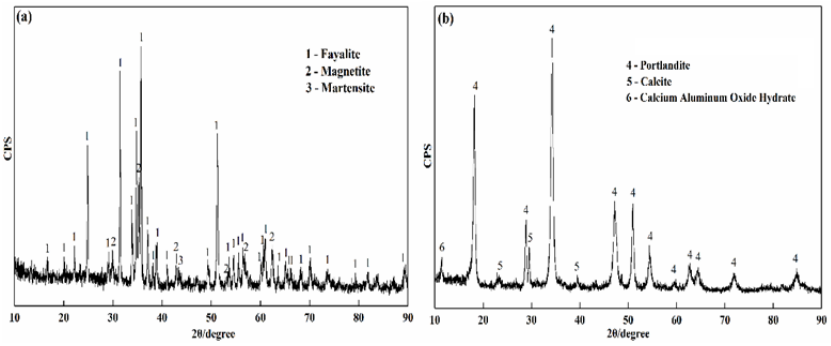

Figure 1: XRD patterns of raw materials: (a) NSS; (b) CCS.

2.2 Experimental Procedure

The Pretreatment of raw materials was refer to previous study. The magnetic product as iron concentrate powder (ICP) was analyzed for iron by the potassium dichromate titration and atomic absorption spectrometry method. The iron recovery was calculated based on the ratio of iron content in iron concentrate powder to that in waste nickel slag. The crystalline and mineral phases were identified by powder XRD patterns using a diffractometer (D/Max-RC, Rigaku, Japan). After embedding samples in resin and polishing, the micro-

morphological observation was carried out using a scanning electron microscope (SEM, EVO-18, Zeiss, Germany) equipped with an energy dispersive X-ray spectrometer (EDS, Quantax, Bruker, Germany).

2.3 Experimental Design

In order to investigate the possible interaction relationship between impact factors on the target responses in DRMS process of NSS, central composite design (CCD) were adopted in this study. Based on the response surface method (RSM), CCD was a widely employed technique for evaluating and optimizing the parameters in process. Compared to the single-factor-at-time experiment, RSM was more appropriate for investigating the optimal value on a certain region efficiently with reducing the experiment time and shortening the experiment cycle (Mu'azu et al., 2014). According to the previous study (Wang et al., 2015), three process factors were determined and limited in a design space, including reduction temperature, reduction time and CCS dosage designated as A, B, C respectively. Each factor was varied over five different levels (coded as -α, -1, 0, 1, α). By the design regulation $\alpha=2^{k/4}$, k meant the number of factors, so k equal to 5 and α equal to 1.682. Owing to the control precision of test equipment, α was valued to two digits after the decimal point for the factors of CCS dosage and reduction time and rounded to the whole number for the factors of CCS dosage and reduction temperature. The impact factors and their coded levels were listed in Table 3. As per the selected design above-mentioned, a total of 20 experiments were required and given in Table 4. Each example in order was correspond to two measured responses: the iron content in the ICP (Y_1) and iron recovery (Y_2). By the statistical software Design Expert version 8, the experimental data were modeled by being fitted into a second order polynomial equation between response and impact factors and the final optimal solutions were obtained.

Table 3: The Actual impact factors and coded values in CCD

Impact Factors	Unit	notation	levels				
			-1.682	-1	0	+1	+1.682
Reduction temperature	°C	A	1032	1100	1200	1300	1368
Reduction time	H	B	0.32	1	2	3	3.68
CCS dosage	mass%	C	30.88	37.65	47.58	57.50	64.27

3. Results and discussion

3.1 Experimental results

Table 4: The design and results of experiments

Number	Impact factors			Results	
	Reduction temperature/ ºC	Reduction time/h	CCS dosage/%	Iron content/%	Iron recovery/%
1	1100	3	37.65	79.05	72.07
2	1300	3	57.50	90.10	91.43
3	1300	3	37.65	86.14	77.17
4	1200	0.32	47.58	56.58	31.22
5	1100	3	57.50	77.47	76.10
6	1300	1	57.50	85.20	77.55
7	1300	1	37.65	87.40	72.76
8	1200	2	47.58	88.53	84.74
9	1200	2	47.58	87.39	85.99
10	1368	2	47.58	88.10	89.20
11	1032	2	47.58	42.38	22.35
12	1200	3.68	47.58	83.09	86.24
13	1100	1	37.65	58.53	44.10
14	1100	1	57.50	55.62	46.00
15	1200	2	64.27	79.07	82.08
16	1200	2	47.58	87.32	87.68
17	1200	2	47.58	88.29	86.97
18	1200	2	47.58	87.28	88.19
19	1200	2	47.58	88.80	86.97
20	1200	2	30.88	77.32	64.39

The results for the measured responses were given in Table 4. As shown in Table 4, the iron content in ICP were ranged between 42.38-90.10 %, which respond to the iron recovery range of 22.35-91.43 %.

It preliminarily indicates that the selected impact factors had great influence on the responses. The fitted second order polynomial models for the iron content in the ICP (Y_1) and the iron recovery (Y_2) are given in equations 1 and 2 respectively. The determination coefficient R^2 indicates the prediction accuracy of the model. The R^2 of the models for Y_1 and Y_2, are 0.9335 and 0.9083 (both close to 1) respectively, which indicates that the predictive values of the model have better correlation with the real values. Also, the precision values of the two models are 11.269 and 10.077 respectively, both greater than 4, which implied that the models had reasonable precision and can be used for analyzation and prediction.

$$Y_1=87.70+11.35A+6.63B+0.016C-4.84AB+0.78AC+0.94BC-6.47A^2-4.84B^2-1.89C^2 \quad (1)$$

$$Y_2=86.48+14.14A+12.37B+4.01C-4.97AB+1.64AC+1.45BC-9.15A^2-8.11B^2-2.98C^2 \quad (2)$$

As the analysis of variance (ANOVA) for the two fitted models were given in Table 5, F values as well as P values of the two models indicated that the different sources of the models' variations can all statistically meet the most significant level. Accordingly, for Y_1 and Y_2, the main factors of A and B, squared terms of A^2 and B^2 had the most significant influence the models' predictions. Differently, the two factors interaction term AB significantly influence model of Y_1 but this interpretation were not deductible for Y_2. Therefore, based on the Table 5, the main effects of A and B were the most significant terms towards iron content and iron recovery while the interacting effects were not revealed the relative importance on the models. Also, both the employing CCD models of Y_1 and Y_2 were capable of providing enough precision for studying and optimizing the effects of investigated impact factors on the selected iron indicators.

*Table 5: ANOVA results of fitted second order polynomial models**

Sources of variance	Y_1: Model of iron content			Y_2: Model of iron recovery		
	F value	P value	Significance	F value	P value	Significance
Model	15.59	<0.0001	***	11.01	0.0004	***
A	71.97	<0.0001	***	37.21	0.0001	***
B	24.57	0.0006	***	28.48	0.0003	***
C	1.36×10^{-4}	0.9909		2.99	0.1144	
AB	7.66	0.0198	*	2.70	0.1315	
AC	0.20	0.6646		0.29	0.5998	
BC	0.29	0.6041		0.23	0.6422	
A^2	24.65	0.0006	***	16.46	0.0023	***
B^2	13.82	0.0040	***	12.92	0.0049	***
C^2	2.10	0.1779		1.74	0.2160	

*Level of significance: *p < 0.05, **p < 0.01, ***p < 0.001.

3.2 Optimization and verification results

With the experimental results above mentioned, the design expert software was employed using the numerical optimization for identifying the optimal reaction conditions for the three investigated factors. Considering the different target optimization requirement, the numerical optimization solutions and results were given in the Table 6. Note that the overall main target goal was to maximize the response Y_1 as well as Y_2 while minimizing or moderating in range the impact factors. The solutions 1-3 were conducted at the minimum value of single factor because the best solution could not be obtained with minimum values of all the investigated factors. Hence, the solution 4 was selected moderately within the range of investigated values, which suggested that the overall optimization reaction conditions were converged at around 1287 ºC, 2.8 h and CCS dosage of 57.19%. Under these optimization reaction conditions, as the parallel verification results were shown in Table 7, the iron content of ICP and iron recovery were reached up to 91.30% and 95.44% respectively, which suggested that the experimental results were basically consistent with the optimization solutions.

*Table 6 : The optimization solutions and results with the different target requirements**

Factor/ response	Unit	Target requirements				Solutions and results			
		1	2	3	4	1	2	3	4
A	ºC	min	-	-	In range	1270.27	1299.78	1295.09	1286.78
B	h	-	min	-	In range	2.99	2.55	2.97	2.80
C	mass %	-	-	min	In range	57.46	57.49	55.54	57.19
Y_1	%	max	max	max	max	90.56	91.54	90.15	91.14
Y_2	%	max	max	max	max	96.36	96.55	95.07	96.69

*Min=minimize, Max=maximize

Table 7：The verification results

Verification orders	Results	
	Iron content/%	Iron recovery/%
1	91.28	95.42
2	91.35	95.38
3	91.29	95.54
Average	91.30	95.44

3.3 XRD Analysis of the reduced samples in PR process

Under the optimization reduction temperature and CCS dosage, the reduced samples in different reduction time were investigated by XRD for analysing phase transitions in the PR process. The XRD patterns of reduced samples at 30 min, 60 min, 120 min, 180 min were given in the in Figure 2. As shown in Figure 2, when reduced at 30 minutes, there are characteristic peak of metallic iron (Fe), ferrowollastonite ($Ca_2Fe_2Si_5O_{14}OH$), kilchoanite ($4CaO•3SiO_2•H_2O$) phase in the XRD patterns. It should be noted that ferrowollastonite is a coexistence phase of wollastonite ($Ca_3(Si_3O_9)$) with relatively higher iron content, which indicated that part of unreduced Fe^{2+} replace the Ca^{2+} in the wollastonite phase as similar as the phase of iron-bearing silicate such as kirschsteinite ($(Ca, Fe)_2[SiO_4]$)and andradite ($Ca_3Fe_2Si_3O_{12}$). With the extension of reduction time, it was the evident that the characteristic peaks of kilchoanite and metallic iron were enhanced while diffraction peaks of ferrowollastonite, kirschsteinite, andradite phase are disappeared because of the iron further reduction.

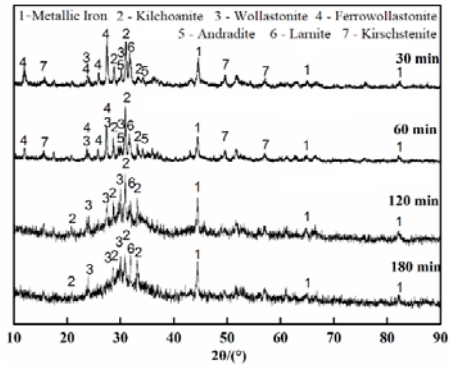

Figure 2：XRD patterns of reduced samples at different reduction time in PR process.

3.4 SEM observation of the optimization sample in PS process

Under the optimal reduction conditions, the SEM image and EDS analyzation of optimization samples in PS process was presented in Figure 3. As shown Figure 3, it can be observed that most of metallic iron phase were effectively separated with silicate slag, and only a little slag phase was covered by the platy iron phase because of ductility. As such, for making the reduction production sample of fine grinding after -0.074 mm accounted for about 90 %, the grinding time (about 45 min) greater than before (30 min). Hence, this implied a further increase of reduction time and temperature could result in lowering the iron recovery.

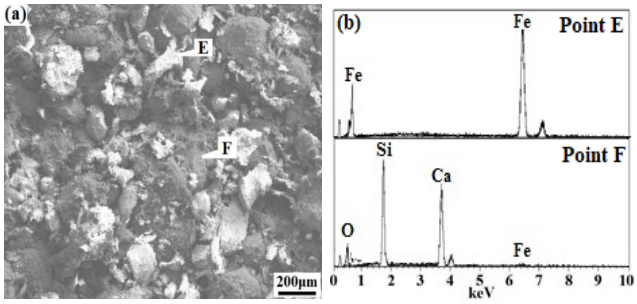

Figure 3：SEM image and EDS analyzation of optimization samples in PS process.

4. Conclusions

(1) Calcium carbide slag (CCS) and coke dust (CD) can be utilized as the additive and the reductant in the direct reduction-magnetic separation (DRMS) process, respectively.
(2) From the result of the RSM, the optimal conditions are at around 1287 ºC, 2.8 h and CCS dosage of 57.19 %. Under these optimization reaction conditions, the iron content of ICP and iron recovery were reached up to 91.30 % and 95.44 % respectively.
(3) The microstructure analysis show that the DRMS process for recovering iron from NSS is reducing the most of the iron oxides from iron-bearing silicate to the metallic iron by the carbon or the carbon monoxide from the gasification.
(4) From SEM images, in the reducing process, metallic iron particles could grow up to form bigger, the small pores gradually merged to form larger and the metallic iron phase could back into the slag phase, which is recommended to further investigate. CCS as additive exerts a great influence on the spatial structure of gas pores in reduction product samples. Under these optimization reduction conditions, the iron phase was separated effectively with the silicate slag in physical separation (PS) process.

Acknowledgments

The authors gratefully acknowledge financial support from China Postdoctoral Science Foundation (2016M602082), supported by Science and Technology Research Project of Higher Education Universities in Hebei Province (ZD2016014, QN2016115), supported by Construction Science and Technology Foundation of Hebei Province (2012-136), supported by Handan Science and Technology Research and Development Plan Program (1621211040-3), supported by Jiangxi Postdoctoral Daily Fund Project (2016RC30).

Reference

Fan D.C., Ni W., Li J., Li Y., Qiu X. J., Fu C.H., Li D.Z., 2015, Generation and reduction mechanism of silicate minerals containing iron in deep reduction of rough concentrate from iron tailings, Journal of Central South University (Science and Technology), 46(6), 1973-1980, DOI: 10.11817/j.issn.1672-7207.2015.06.001.

Han Y.X., Zhang C.W., Sun Y.S., Gao P., 2012, Mechanism analysis on deep reduction of complex refractory iron ore promoted by Na_2CO_3, Journal of Northeastern University (Natural Science), 33(11), 1633-1636.

Jia Y., Ni W., Wang Z.J., Gao S.J., Feng J.P., 2011, Deep reduction experiments of bayer red mud for iron recovery, Journal of University of Science and Technology Beijing, 33(9), 1059-1064, DOI: 10.13374/j.issn1001-053x.2011.09.007.

Li K.Q., Ping S., Wang H.Y., Ni W., 2013, Recovery of iron from copper slag by deep reduction and magnetic beneficiation, Journal of Minerals, Metallurgy and Materials, 20(11), 1035-1041, DOI: 10.1007/s12613-013-0831-3.

Li Y.J., Li S.F., Han Y.X., 2011, Deep reduction/magnetic separation of laterite for concentration of Ni and Fe, Journal of Northeastern University (Natural Science) ,32(5), 740-744.

Mu'azu N.D., Al-Malack M.H., Jarrah N., 2014, Electrochemical oxidation of lowphenol concentration on boron doped diamond anodes: optimization viaresponse surface methodology, Desalination and Water Treat, 52(37-39), 7293–7305, DOI: 10.3303/CET0918162.

Wang C.L., Wang S., Qiao C.Y., Ni W., Xu C.Y., Qiu X.J., Ping S., 2014, Effects of coal types on iron recovery from iron ore tailings with high iron silicate by deep reduction process, Transactions of Materials and Heat Treatment, 35(9), 16-22, DOI: 10.13289/j.issn.1009-6264.2014.09.004.

Wang S., Ni W., Li K. Q., Wang C. L., Wang J. Y., 2014, Effect of basicity on recovering iron, nickel and copper by deep reduction process of nickel slag pellets, Transactions of Materials and Heat Treatment, 35(9), 23-28, DOI: 10.13289/j.issn.1009-6264.2014.09.005.

Yu W., Sun T. C., Cui Q., Xu C.Y., Kou J., 2015, Effect of coal type on the reduction and magnetic separation of a high-phosphorus oolitic hematite ore, ISIJ International, 55(3), 536-543, DOI: 10.2355/isijinternational.55.536.